Control strategies for a micro-conveyance system based on an electromagnetic digital actuator array

S Duque Tisnés, L. Petit, Christine Prelle

Control strategies for a micro-conveyance system based on an electromagnetic digital actuator array

S. Duque Tisnés, L. Petit, C. Prelle
CNRS, FRE 2012 Laboratoire Roberval, Sorbonne universités
Université de Technologie de Compiègne (UTC)
60203 Compiègne, France
sduqueti@utc.fr

***Abstract*— In this paper we present two different control strategies to ensure the trajectory and final position of a transported object in a micro-conveyance system. This system is oriented towards a micro-factory application. The conveyance system is based on a 5x5 matrix array of electromagnetic digital actuators. Each actuator has two DOF and four discrete positions. The digital actuator uses the Lorentz force generated by two pairs of orthogonal wires to move its mobile part. Permanent magnets surrounding each actuator ensure the preservation of the discrete positions. The collaborative action of the actuators produces the conveyance of objects on the system thanks to friction phenomena. A dynamic model of the object's displacement is presented and used to generate the object's trajectories. The performance of the control strategies is simulated and compared. The conveyance is attained with a speed of 0.63 mm/s and sub-micrometer tolerances consuming 1.44 J/mm.**

Keywords—conveyance system, micro-factory, discrete actuator, collaborative actuation, open-loop trajectory control, MEMS array

I. INTRODUCTION

The interest for smaller devices in engineering has driven attention to the miniaturization of products, reaching the micro and nano scales. From this need, the concept of micro-factory was born, aiming to develop machining tools of the size of the produced goods to reduce the energy consumed and production costs [1]. A critical element of a modern factory is its transportation system. From raw material to final product, multiple objects need to be conveyed between different machining stations and quality control stages until the transformation is done and the desired product manufactured. In the case of a micro-factory, the high density of stations in a compacted structure increases the importance of an autonomous, flexible, precise and easy to integrate conveyance system (conveyor).

Different transportation systems with micrometer precision have been presented in the literature. They can be classified by the kind of energy used for the displacement: pneumatic [2]–[4], electromagnetic [5], [6], and electrostatic [7], [8]. All these systems are based on an analogical actuation principle, i.e. a continuous movement of the object in the actuator's stroke is expected and they use closed loops controls to reach high performance levels, thus needing sensors and dedicated electronics. As an alternative, conveyance systems based on a collaboration of digital actuators have been proposed [9]–[11]. These systems use electromagnetic, electrostatic, thermal or pneumatic energy to perform the movement of the conveyed object with a series of transitional states. Also, the discrete positions attained by the actuator are "stable" positions, i.e. no energy is required to maintain them [12]. The initial and final position of the digital actuators are assured by a holding force and the intermediate states predicted by a dynamic model, allowing the conveyor to be implemented in open loop control [13]. This avoids the need for sensors and dedicated electronics, simplifying the conveyor's integration in the micro-factory context. The open loop control enables the use of pulsing signals, reducing the energy needed to control the system. On the other hand, the fabrication process of the actuator is a critical issue as it defines the actuator's stroke. Errors cannot be corrected by a closed loop control as there is no sensor. Also, the dynamics of the conveyed object is discrete, that is, displaced step by step [14].

In this work, we present a 2D micro-conveyance system based on a 5×5 matrix array of electromagnetic digital actuators with four discrete positions. As each actuator has two degrees of freedom, complex trajectories and multiple combinations of movements can be accomplished with the array. A model of the object's displacement is described and used to generate its possible trajectories. Finally, two different kinds of control strategies, based on the dynamic model are developed and their simulated performances presented.

II. PRINCIPLE OF THE CONVEYANCE SYSTEM

A. Principle of the Elemental Digital Actuator (EDA)

The Elemental Digital Actuator (EDA) is composed of 5 gold-coated neodymium Permanent Magnets (PMs). The center PM is the mobile part of the actuator, the Mobile Permanent Magnet (MPM), and it is placed into a square cavity. The square cavity (2.2 × 2.2 mm) is slightly larger than the MPM cross section (2.0 mm × 2.0 mm). This small gap represents the actuator's stroke in both x and y directions (0.2 mm). The other four PMs are fixed around the square cavity, therefore named Fixed Permanent Magnets (FPMs), each at the same distance "*d1*" (Fig. 1, Table I). The FPMs are 1 mm long (along z-axis) while the MPM is 1.2 mm. This difference ensures that, when a rigid object lies on top of the EDA, the MPM is the only contact between the device and the conveyed object. The orientation of the magnetization of the MPM and FPMs is such that an

attracting magnetic force exists between MPM and each FPM, creating five possible equilibrium positions:

- Each corner of the cavity, where there is mechanical contact between the MPM and the cavity's walls
- The center of the EDA, where the four magnetic forces between the MPM and FPM compensate each other, i.e. a critical equilibrium point.

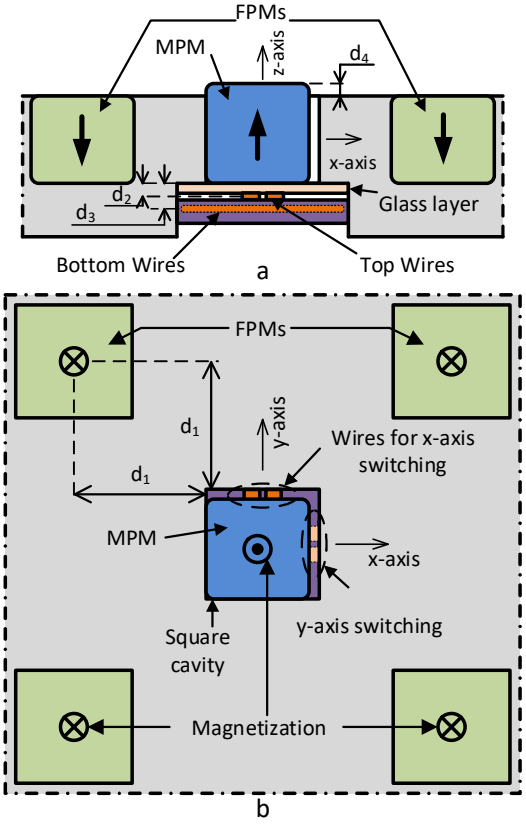

Fig. 1.Schematic Side (a.) and Top (b.) views of the Elemental Digital Actuator (EDA).

Table I. EDA CHARACTERISTICS TABLE

PMs Structure		NdFeB Silicon	
PM	Dimensions (mm)	Magnetization (T)	Mass (g)
MPM	2.0 × 2.0 × 1.2	1.22	0.034
FPM	2.5 × 2.5 × 1.0	1.43	0.045
Static friction coefficients: Silicon-MPM 0.38, Glass-MPM 0.26			
d_1		2600 µm	
d_2		117.5 µm	
d_3		252.5 µm	
d_4		200 µm	
Stroke		200 µm	

Only the four corners of the MPM's cavity are the considered discrete positions of the actuator, explaining its digital nature.
To actuate the MPM, two pairs of wires are placed under the cavity. When an electrical current passes through the wires, an electromagnetic force (Fem) (Lorentz Force) appears between the MPM and the wires [15]. As the Lorentz Force generated by wires is orthogonal to them, the wires placed along the x-axis switch the MPM in the y-axis and vice versa.
When a current is injected to displace the MPM, the current is called the Driving Current (I_d). During a switch in one direction (for example along the x-axis) a second current, called the Holding Current (I_h), can be injected in the x-axis wire to generate an Fem along the y-axis and increase the contact force between the MPM and the side of the cavity. This can be useful to ensure the straightness of movement along the MPM trajectory. To avoid electrical contact between the two orthogonal wires, they are in different planes of a Printed Circuit Board (PCB) so that they are at different distances from the MPM. The wires close to the MPM are called Top Wires (TW) and the other pair Bottom Wires (BW). The TW switches the MPM in the x-axis and the BT in the y-axis (Fig. 1).
Finally, a thin glass layer is placed between the MPM and the TW to avoid their direct contact and give the MPM a plane surface to slide between the discrete positions.

B. Principle of the actuator array

The Digital Actuator Array (DAA) consists of 5×5 EDAs arranged in a square matrix with two adjacent EDAs sharing a pair of FPMs to decrease the DAA size (Fig. 2). This array includes a new kind of PM; the Balancing Fixed Permanent Magnets (BFPMs), to ensure that the behavior of the DAA is homogeneous in terms of magnetic force for each EDA.
One of the proposed applications of the DAA is as a conveyance system, in the micro-factory environment [9].

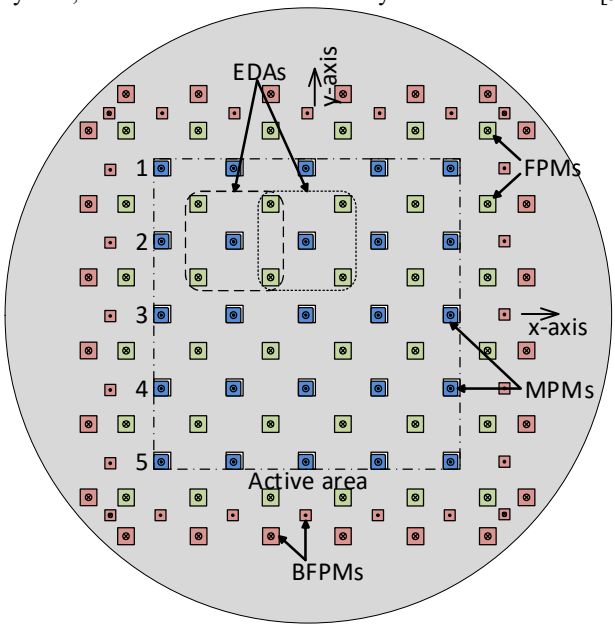

Fig. 2. Top view of the Digital Actuation Array (DAA) in a 4" silicon wafer, MPMs are blue, FPMs are green and the red ones are BFPMs.

In Fig. 3. The DAA is viewed from a cross section perspective showing only the MPMs, their cavities and the conveyed object: a 0.7 g, 130 µm thick glass layer. To transport an object, the DAA uses the following principle: the conveyed objects rest on

top of the MPMs, which are in an initial position (Step a). They are activated simultaneously to displace the object (Step b). The friction force between the MPMs and the carried object displaces the object until the MPMs reach the stroke distance. Once the MPMs stop, the dynamic friction due to the relative movement of the accelerated object and the static MPMs act as a brake to the object until it stops, reaching a "quantum" of displacement. The second phase "Slip" begins to reset the configuration for a new Step a: each MPM is activated individually to return to its initial position (Steps c to e). The friction force between a single MPM and the object is inferior to the opposition force of all the other MPMs. Thereafter, the MPM slides without moving the object and a new "quantum" step can begin when all the MPMs are back to the initial position (Step a).

As the current needed to return the MPMs to the initial position has a different sign of the driving current (I_d), it is noted as return current (I_r) in Fig. 3.

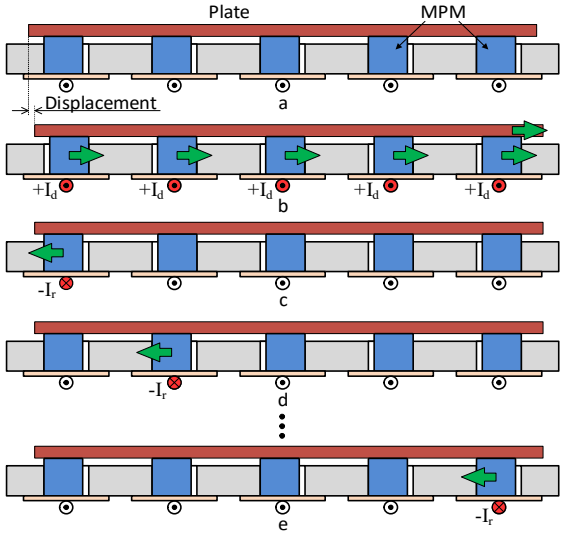

Fig. 3. Principle of conveyance of the DAA by collaborative effort of the MPMs and individual return of each one (quantum step).

III. Displacement Model

A. Static model

The magnetic and electromagnetic forces acting on the MPM were computed using the semi-analytical computing software RADIA, which is based on Mathematica and dedicated to 3D magnetostatics computation. These forces were computed for a series of (x, y) coordinate pairs in the actuator's cavity. The center of the coordinate system is the middle point of the EDA's cavity. Once the value of the magnetic and electromagnetic forces for these points was obtained, a polynomic interpolation was done to obtain a continuous function of them in $x, y,$ and z directions.

The magnetic attracting force between the MPM and the FPMs as a function of the MPM's position in the cavity (x or y axis as the EDA is symmetric) is linear, with absolute value of 0.43mN at the discrete positions. Fig. 4 shows the electromagnetic force generated by the BW and TW onto the MPM as a function of the MPM's position. The difference between the curves is due to the distance of the BW and TW to the MPM, as explained in II.A. This means that the activation of the EDA along the x-axis is not symmetric to the y-axis, for the same driving current. The TW curve is along the x-axis position and the BW is along the y-axis position. Finally, a parabolic form is observed in the curves, more notably in the BW than the TW. This follows the Lorentz force formula and the difference in distances between the BW to the MPM and the TW to the MPM [15].

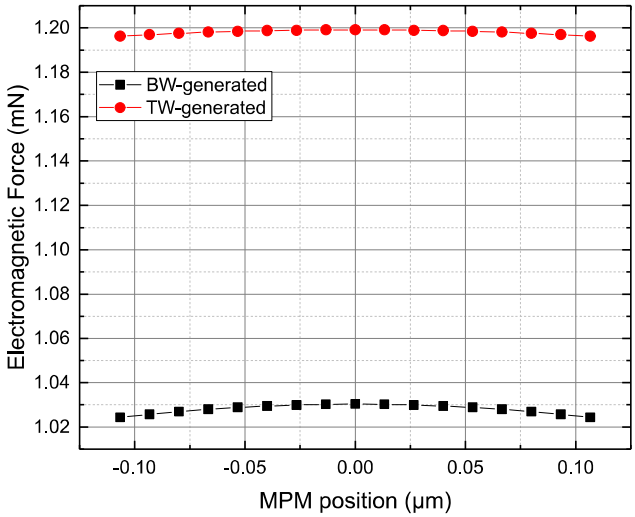

Fig. 4. Electromagnetic force due to the BW and TW onto the MPM for a 1 A I_d current and its polynomial interpolation.

Table II. MAGNETIC & ELECTROMAGNETIC FORCE MAGNITUDES

Magnetic Holding Force in Discrete Positions (mN)	0.43
Driving Force TW (mN/A) for the (0,0) MPM's position	1.20
Driving Force BW (mN/A) for the (0,0) MPM's position	1.03

The magnetic force is the result of the geometry and magnetization values of the EDA. The electromagnetic forces, called Driving Forces in Table II, are the control variables of the EDA and change with the current value injected in the TW and BW. i.e. I_d or I_h as explained in II.A.

B. Dynamic model: elemental and global

A dynamic model, based on the static model, was developed to predict the movement of the MPM between two discrete positions of a single EDA. This model is the Elemental Dynamic Model (EDM). This EDM considers: the duration and shape of the I_d and I_h currents, the friction phenomena between the MPM with the bottom and lateral surfaces of the cavity, the fraction of the conveyed object on top of the EDA (mass) and the friction phenomena between this object and the MPM. The friction phenomena are the transfer of energy to the object by the MPM and its sliding until rest once the MPM has stopped. The EDM is based on Newton's Second Law and the Coulomb friction model. As shown in Fig. 5 for a 0.7 g object, the MPM movement is constantly accelerated by the constant value of I_d.

The MPM transfers energy to accelerate the fraction of the object on top of it by friction until it reaches the stroke (t =2.28 ms). The MPM collides with the cavity's wall and stays in the discrete position but the object slides on top of it and the friction between it and the MPM top surface acts as a brake. When the object stops the system has performed a quantum displacement (t =5.53 ms).

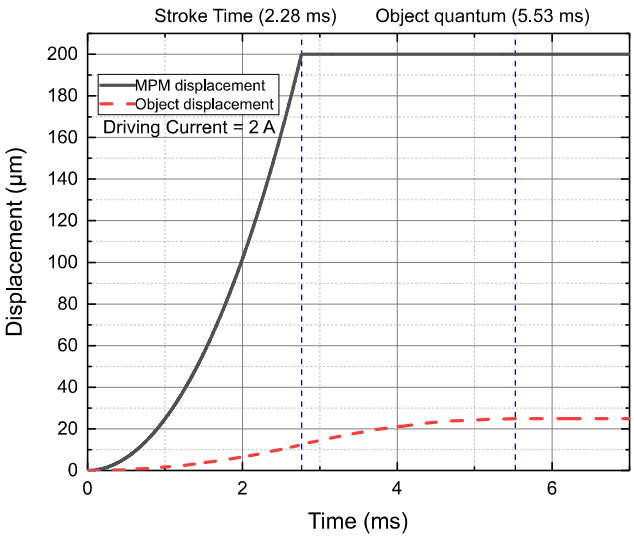

Fig. 5. MPM and Object displacement calculated by the model for a 2 A I_d without Holding Current.

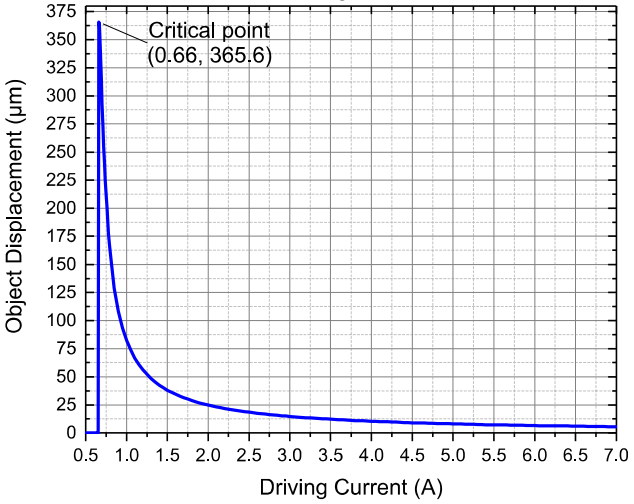

Fig. 6. Object displacement vs I_d as predicted by the model for 25 EDAs and no I_h. Critical point as the F_{em} beats the friction and magnetic forces.

With this EDM, a Global Dynamic Model (GDM) was built assuming that all 25 EDAs in the DAA are identical and contribute equally to the movement of the conveyed object. Then, the displacement of the conveyed object in function of I_d was computed as shown in Fig. 6. The displacement decreases with the value of I_d as the MPM acceleration is greater and the amount of energy transferred to the object through friction is reduced. It is important to observe the critical point at which the F_{em} generated by the I_d exceeds the magnetic and static friction forces of the system and the EDAs are activated. Finally, a last control variable was considered: The Number of Activated EDAs (N_a). With fewer EDAs activated, for a constant I_d value, a smaller displacement is obtained as the non-activated EDAs act as a break. i.e. they add opposing friction forces to the object. This means that the minimum N_a to obtain an object displacement is half the total number of EDAs plus one (N_a = 13 for the considered DAA), as the generated displacement friction needs to be greater than the breaking friction to start the displacement.

IV. Trajectory Algorithm and Control Strategies

A. Description of the conveyance control strategies

Based on the GDM, we constructed a trajectory algorithm that takes the initial and final position of the object and computes the path between them. To follow this trajectory, we developed two different conveyance strategies. These conveyance strategies are called control strategies as they define the control parameters of the DAA for each step. Three parameters were defined as the performance criteria to evaluate the control strategies: conveyance duration, electrical energy consumption and final position precision (due to the discrete displacement and tribology effects).

1) Control strategy 1 (Strategy 1):

This executes the system's maximal displacement as long as possible and then, once the object arrives in the neighborhood of the wished position, it executes a small step varying the control parameters to attain the final position. The maximal displacement combination of I_d, I_h, N_a is the critical point shown in Fig. 6. This is when the Fem is just greater than the magnetic and the friction forces. Due to the heterogeneity of the friction on the surfaces at the microscopic level, this critical point could slightly change between the EDAs. If the same control variables of this critical point are used for all the EDAs, the displacement could not occur as the contributed action of the DAA is lost. To avoid this experimental problem, a safe margin in terms of a minimum value of I_d was defined for all the strategies, in this case a 2A value.

2) Control strategy 2:

This divides the distance into an integer number of identical displacement steps. With this strategy there is no need to adjust the final step of displacement, but the wished distance is not always a multiple of the DAA possible steps, so a tolerance of 0.1 µm in the final position (0.05% of the stroke distance) was considered to develop the strategy. The division can be optimized for each of the three performance criteria defined: consumed energy, conveyance time and final position error. As the tolerance is small compared to the displacement that the DAA could generate, the required displacement steps are minor and thus the control variables remain above the critical point, so it would work experimentally. Moreover, constant values of I_d and I_h are found for each performance criterion, opening the door to an easier electronic implementation for the experimental set-up. Therefore, Strategy 2 finds three possible solutions (I_d, I_h, N_a): to obtain the minimum error (Strategy 2

Min Error), minimum energy (Strategy 2 Min Energy) or minimum transport time (Strategy 2 Min Time), the latter two within the tolerance defined.

The two strategies are illustrated in Fig. 7, with s the step size and d the total desired conveyance distance:

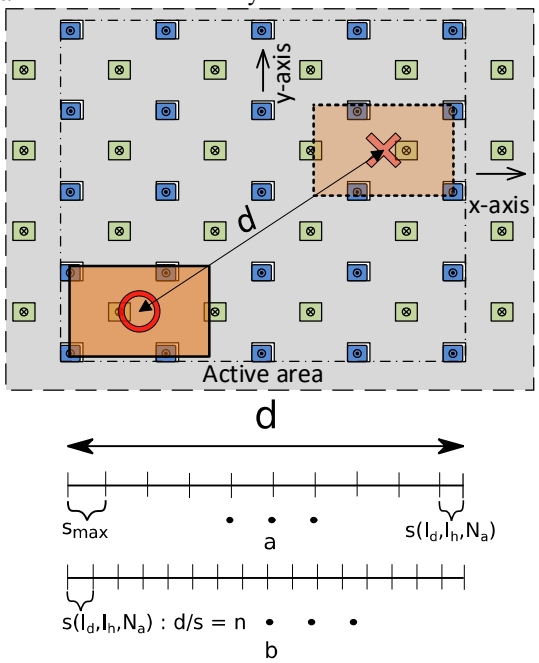

Fig. 7. Control Strategies comparison: (a) Strategy 1 with maximum object displacement s_{max} and a correction step $s(I_d, I_h, N_a)$ at the end. (b) a calculated $s(I_d, I_h, N_a)$ to divide d in an integer number of steps n.

B. *Simulation results*

The two control strategies were simulated for different conveyance distance values along the x-axis. The objective was to compare the performance of the strategies and evaluate the DAA as a conveyance system.

The control variables used by the strategies for the presented simulations were I_d and N_a. Constant values of I_d were used during the step of the MPMs. No I_h was used as it would increase the energy and time consumed for the displacements. A 0.7 g object was simulated on top of the system.

Fig. 8 shows the consumed energy as a function of the conveyed distance for Strategy 1 and Strategies 2, following the equation $E = I^2 R\, T_s$ with I the driving current, T_s the stroke time and R a reference value of 1 ohm for comparison. Strategy 1 is the most efficient as it uses the biggest possible steps, i.e. the minimum I_d available, and it adjusts the position only in its final step. The opposite is Strategy 2 Min Error, as it uses finer steps to arrive nearer the wished destination and thus, a higher I_d for more steps. Strategy 1 seems to have a linear tendency, but in fact it doesn't; the final step is a correction that varies for different values of distance. As it is only a single step of variation, the difference with a straight line is very small. The other two Strategies 2 (Min Energy and Min Time) are very similar in performance, as the energy consumed is linked to the stroke time. The time taken to reach different transportation distances for each strategy implemented is represented in Fig. 9. Again, Strategy 1 is the most efficient and Strategy 2 Min Error is the slowest. The reason, again, is that strategy 1 takes fewer, bigger steps in contrast to the numerous, finer steps of Strategy 2 family.

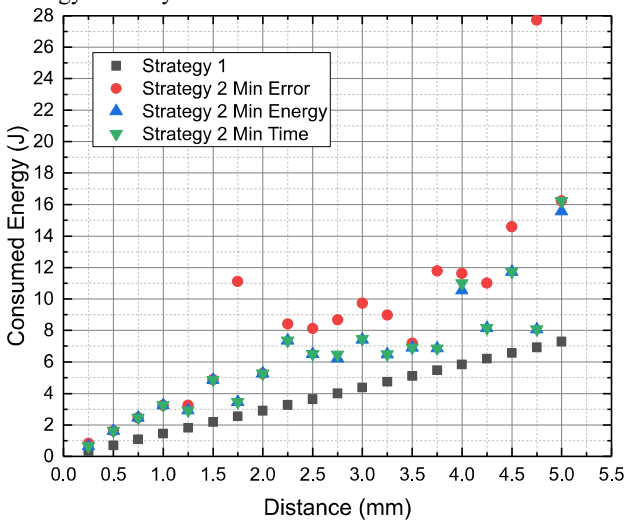

Fig. 8. Consumed energy vs conveyed distance (simulated results).

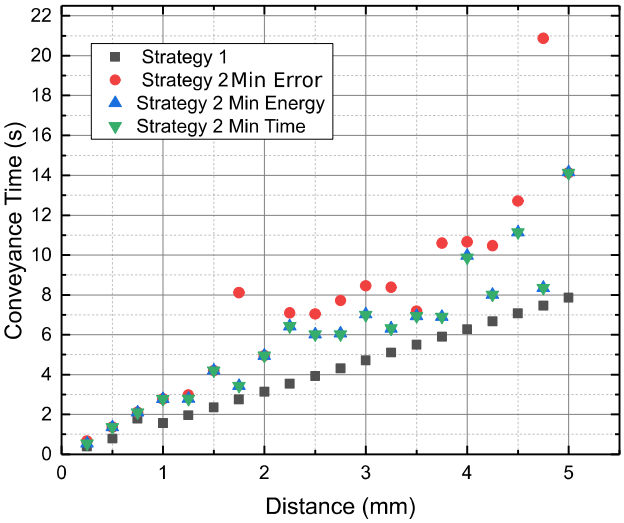

Fig. 9. Conveyance time taken by each strategy for different conveyed distances (simulated results).

To illustrate the different I_d values between the strategies, the 4 mm conveyance distance solution is detailed in Fig. 10. Strategy 1 takes a small I_d (2 A) for 175 steps using all 25 EDAs, and then computes the control variables to attain the final position with its final step ($I_d = 2.14$ A, $N_a = 21$). Strategy 2 Min Error takes a high I_d (2.94 A) to execute smaller steps to reach the final position as close as possible (in 317 steps), using 24 EDAs. This explains the longer time and the higher energy shown in Fig. 8 and Fig. 9 for Strategy 2 Min Error compared to Strategy 1. The other Strategy 2 solutions differ significantly. The Min Energy uses 24 actuators and chooses a high I_d value (2.99 A) for the smallest number of

steps of the strategy 2 family (287). Min Time uses 21 actuators and a smaller current (2.11 A) but for longer (328 steps). Nevertheless, they have a very similar performance overall, as seen in Table III.

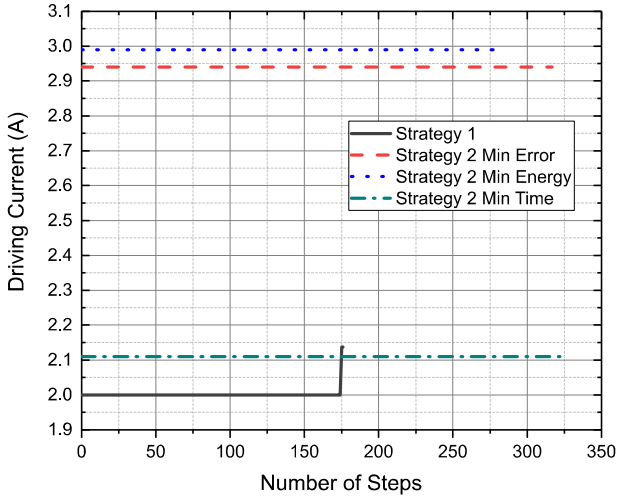

Fig. 10. I_d difference for a 4 mm displacement.

The potential performance of the DAA as a conveyance system with the implemented control strategies are listed in Table III.

Table III. DAA SIMULATED PERFORMANCE RESULTS

	Energy/distance (J/mm)	Speed (mm/s)	Error (m)
Strategy 1	1.44	0.630	0
Strategy 2 Min Error	3.35	0.360	1e-9
Strategy 2 Min Energy	2.54	0.436	1e-7
Strategy 2 Min Time	2.56	0.437	1e-7

As presented, the optimal solution for these three criteria is Strategy 1, being the fastest and less consuming alternative and attaining the final position with a theoretical zero error but needing a variable I_d value. Strategy 2 family offers different local optimum for the desired distance to travel; min error, time or energy, but it compromises the other two criteria. Nevertheless, Strategies 2 execute smaller steps than Strategy 1, (using a higher I_d) so they would have a smaller error with the wished trajectory (a line) than Strategy 1.

V. CONCLUSION AND PERSPECTIVES

In this paper, a micro-conveyance system based on a digital actuator array was presented. Its working principle was explained from the electromagnetic nature of the elemental component of the array to the friction-driven method of transportation. A displacement model for the conveyed object and mobile part of the system was described and implemented to develop two different control strategies. The performances of these control strategies were evaluated and presented as a function of three defined criteria: error in the final position, energy consumed and time taken to attain the final position. Finally, a performance optimum for these criteria was found in Strategy 1. Possible implementation advantages were discussed for Strategy 2 family, mainly a smaller trajectory error and a reliable operation. The maximal simulated speed of the conveyor was 0.63 mm/s with an energy consumption of 1.44 J/mm and with zero theoretical error. Future work will be centered in a fourth performance criterion, the trajectory deviation of the object. Afterwards, the simulation will be compared with experimental measurements. It is also planned to evaluate the influence of the third control variable (I_h) and the sensibility of all parameters of the dynamic model.

ACKNOWLEDGMENT

This work is supported by a public grant overseen by the French National Research Agency (ANR) as part of the "Tridimensional micro-conveyance systems for micro-factory" program (ANR-15-CE10-0002-01).

REFERENCES

[1] Y. Okazaki, N. Mishima, and K. Ashida, "Microfactory—Concept, History, and Developments," *J. Manuf. Sci. Eng.*, vol. 126, no. 4, p. 837, 2004.

[2] R. Yahiaoui, R. Zeggari, J. Malapert, and J. F. Manceau, "A MEMS-based pneumatic micro-conveyor for planar micromanipulation," *Mechatronics*, vol. 22, no. 5, pp. 515–521, 2012.

[3] A. Delettre, "Conception, modélisation et commande d'une surface de manipulation sans contact à flux d'air induit.," Université de Franche-Comté, 2011.

[4] R. Yahiaoui, R. Zeggari, J. Malapert, and J. F. Manceau, "A new two-dimensional actuator for air flow micro-manipulation," in *Proceedings - 2010 First Workshop on Hardware and Software Implementation and Control of Distributed MEMS, dMEMS 2010*, 2010, pp. 11–15.

[5] G.-Z. Cao, J.-L. Fang, S.-D. Huang, J.-A. Duan, and J. F. Pan, "Optimization Design of the Planar Switched Reluctance Motor on Electromagnetic Force Ripple Minimization," *IEEE Trans. Magn.*, vol. 50, no. 11, pp. 1–4, 2014.

[6] Ž. V. Despotović, D. Urukalo, M. R. Lečić, and A. Ćosić, "Mathematical modeling of resonant linear vibratory conveyor with electromagnetic excitation: simulations and experimental results," *Appl. Math. Model.*, vol. 41, pp. 1–24, 2017.

[7] X. Li and A. Yamamoto, "A Multi-slider Linear Actuator Using Modulated Electrostatic Attraction and Inertia Effect," in *Mecatronics - REM*, 2016, pp. 296–301.

[8] D. V. Dao, P. H. Pham, and S. Sugiyama, "Multimodule micro transportation system based on electrostatic comb-drive actuator and ratchet mechanism," *J. Microelectromechanical Syst.*, vol. 20, no. 1, pp. 140–149, 2011.

[9] Z. Shi *et al.*, "Development of an elementary micromachined electromagnetic digital actuator for microdisplacements," in *Symposium on Design, Test, Integration & Packaging of MEMS and MOEMS*, 2016, pp. 2–5.

[10] L. Petit, E. Dupont, E. Doré, F. Lamarque, and C. Prelle, "Design and Characterization of a High-Precision Digital Electromagnetic Actuator with Four Discrete Positions," *Actuators*, vol. 4, no. 4, pp. 217–236, 2015.

[11] Y. A. Chapuis, L. Zhou, Y. Fukuta, Y. Mita, and H. Fujita, "FPGA-based decentralized control of arrayed MEMS for microrobotic application," *IEEE Trans. Ind. Electron.*, vol. 54, no. 4, pp. 1926–1936, 2007.

[12] B. D. Jensen, A. A. Mi, L. L. Howell, M. B. Parkinson, A. A. Mi, and M. S. Baker, "DESIGN OPTIMIZATION OF A FULLY-COMPLIANT BISTABLE MICRO-MECHANISM," in *ASME International Mechanical Engineering Congress and Exposition*, 2001, pp. 1–7.

[13] X. Liu *et al.*, "An optical wireless bistable micro-actuator," *2015 IEEE Int. Conf. Mechatronics Autom. ICMA 2015*, pp. 1624–1629, 2015.

[14] P. Chouinard and J. S. Plante, "Bistable antagonistic dielectric elastomer actuators for binary robotics and mechatronics," *IEEE/ASME Trans. Mechatronics*, vol. 17, no. 5, pp. 857–865, 2012.

[15] E. P. Furlani, *Permanent Magnet And Electromagnetical Devices*, Academic P. Rochester, New York: Elsevier, 2001.